2013 International Nuclear Atlantic Conference - INAC 2013
Recife, PE, Brazil, November 24-29, 2013
ASSOCIAÇÃO BRASILEIRA DE ENERGIA NUCLEAR - ABEN
ISBN: **978-85-99141-05-2**

STUDY ON THE MICROSTRUCTURE OF RECYCLED ZIRCALOY BY X-RAY DIFFRACTION LINE PROFILE ANALYSIS

Rodrigo U. Ichikawa[1], Luiz A. T. Pereira[1], Kengo Imakuma[1], Xavier Turrillas[2] and Luis G. Martinez[1]

[1] Nuclear and Energy Research Institute (IPEN / CNEN - SP)
Av. Professor Lineu Prestes 2242
05508-000 São Paulo, SP, Brazil
ichikawa@usp.br ; luiz.atp@uol.com.br ; kimakuma@ipen.br ; lgallego@ipen.br

[2] Materials Science Institute of Barcelona -ICMAB and ALBA Synchrotron Light Source
Campus UAB, Bellaterra 08193, Barcelona, Spain
xturrillas@icmab.cat

ABSTRACT

In the fabrication of nuclear fuel elements parts, Zircaloy machining chips are generated and, as this material is high-valued and controlled, its recycling presents high interest not only in economic aspects but also for environmental reasons and due to its strategic role in nuclear technology. Two processes for the recovery of these Zircaloy chips are being studied at IPEN-CNEN/SP. One of the processes is by conventional remelting of the material in a VAR (Vacuum Arc Remelting) furnace for producing solid ingots. Concurrently it is being studied an alternative process, by powder metallurgy methods, by which the chips are hydrided in order to become brittle and be grinded. The resulting ground powder is then compacted and finally vacuum-dehydrided and sintered in one step to form solid pieces. The VAR-remelted samples were also submitted to heat treatments in order to refine their microstructures, resulting in three different samples named “as cast”, “annealed” and “tempered”. The microstructures resulting from both processes and also from heat treatments were studied by metallography and X-ray diffraction (XRD). In this work, results of a XRD study are presented applying X-ray diffraction Line Profile Analysis (XLPA) methods in order to determine the mean crystallite sizes and the RMS microstrains on these samples. Additionally, a study for verify the influence of different standard materials used for the correction of the instrumental breadth in the XLPA was developed. The XLPA results show the influence of the processes and also of heat treatments on mean crystallite sizes and microstrains of the samples and were compared to their metallographic study and hardness.

1. INTRODUCTION

In PWR and BWR nuclear power reactors, the fuel is composed of uranium dioxide pellets conditioned in cladding tubes, forming the fuel rod. A set of fuel rods, disposed in an assembly, forms the fuel element. The cladding and the structural materials of the fuel elements have to present very specific mechanical, corrosion and nuclear properties. The materials which best meet these requirements are the zirconium alloys, so-called Zircaloys. The processes of fuel elements fabrication generate machining chips which cannot be discarded as ordinary scrap, once nuclear grade Zircaloy is considered a controlled material, besides being pyrophoric and presenting high costs of production. Furthermore, the fabrication of these alloys demands high consumption of energy and highly controlled processes. Therefore, the recycling of Zircaloy scraps presents great economic and environmental relevance. Particularly for the Brazilian case, in addition to the economic and environmental interests, there is a strategic aspect to be considered, once Brazil does not produce zirconium alloys at industrial scale.

In order to develop processes for recycling the Zircaloy scraps generated from the fabrication of fuel elements for the Brazilian reactors by the Indústrias Nucleares Brasileiras - INB, a research program is being developed at the Instituto de Pesquisas Energéticas e Nucleares – IPEN-CNEN/SP [1-6]. There are two routes being studied for this purpose: by vacuum arc remelting (VAR) and by hydriding/sintering processes. In both processes, it is necessary to ensure that the composition of the alloy is neither changed nor contaminants are introduced and equally ensure that the microstructure of the alloy is appropriate. Therefore, besides the development of these processes on itself, the establishment of methodologies for the characterization of the products is of paramount importance [1,2].

The details of the processes, results for chemical composition and metallographic analyses of the samples produced by both processes were already described in previous works [1-6]. In this work is presented a study of the microstructures of samples produced by these processes, performed by X-ray diffraction techniques, especially by X-ray diffraction Line Profile Analysis (XLPA).

The XLPA methods allow determining the mean crystallite sizes and microstrains due to defects in the crystal structure. X-ray line profile analysis methods are being increasingly used due to its simplicity in the sample preparation, data acquisition and capacity of analyze a large area of the material providing better statistical results. For a more elaborated analysis the diffraction pattern can be studied by its Fourier coefficients where no assumptions on the shape of the profiles are made, i.e. the so-called Warren-Averbach Fourier space method. For simpler analysis the full width at half maximum (FWHM) or the integral breadth of only one reflection profile is sufficient. In these methods, known as Single Line method, the profiles are approximated to analytical functions and are known as real space methods.

2. EXPERIMENTAL

The Zircaloy machining chips were provided by Indústrias Nucleares Brasileiras – INB, resulting from the process of fabrication of end-caps for the fuel cladding. The recycled samples were obtained by two different processes: VAR-remelting and powder metallurgy.

The VAR-remelted sample presents a microstructure characteristic of the rapid solidification of the material from melting and was named “as-cast” sample (AC). In order to homogenize the microstructure, heat treatments were performed at 1000° C / 2 h with two different cooling rates. One of the heat-treated samples was water-quenched from the heat-treatment temperature and was called “tempered” (TEMP). Other heat-treated sample was kept to slow cooling in the furnace and was called “annealed” (ANN) [1-6]. The sample produced by powder metallurgy, as described in previous works [2-5], was named “sintered” (SINT) and, as it presents homogeneous microstructure, was used as a standard for the correction of the instrumental profile breadth, as it will be described in the following sections.

The XRD measurements were performed at a Rigaku, model ULTIMA-IV, X-ray diffractometer, equipped with a scintillation detector and a pyrolitic graphite monocromator, using Cu-Kα radiation. It was used a goniometer of 285 mm radius in Bragg-Brentano geometry and X-rays beam slits of ½°, 0.6 mm, ½° and 10 mm (divergence, receiving, scatter and length slits, respectively). The XRD profile was measured at a power of 40 kV and 30 mA in 0.01° steps and step-counting times varying from 10 to 100 s in order to ensure good

counting statistics. The reflection (101) was used for the Single-Line method and the reflections (101) and (202) were used for the Warren-Averbach method.

For the determination of instrumental broadening of XRD profiles, two materials were employed as standards: the sintered Zircaloy and a Y_2O_3 Standard Reference Material for powder diffraction [7]. Both standards present narrow XRD profiles and were tested for studies of the influence of the standard on the results.

3. METHODS

In this work two XLPA methods were applied: the Single-Line (real space method) and the Warren-Averbach (Fourier space method). The theory of the methods is presented briefly in the next paragraphs.

3.1. Single-Line Method

In this method the diffraction profile is approximated by a Voigt function, which is the convolution of a Cauchy function and a Gaussian. Langford [10] showed that the convolution of m Cauchy functions and n Gaussian functions are given by:

$$\beta_C = \sum_{i=1}^{m} \beta_{Ci} \tag{1}$$

$$\beta_G^2 = \sum_{i=1}^{n} \beta_{Gi}^2 \tag{2}$$

Where β_C and β_G are the integral breadths of the Cauchy and Gaussian functions respectively.

If we consider that the measured profile (h) is the convolution of two other profiles, the physical profile (f) and the profile of the instrumental contribution (g) we have [11]:

$$h_C = g_C * f_C$$

$$h_G = g_G * f_G$$

From Eqs. (1) and (2) considering that $m = 2$ and $n = 2$, it follows that:

$$\beta_C^f = \beta_C^h - \beta_C^g \tag{3}$$

$$\left(\beta_G^f\right)^2 = \left(\beta_G^h\right)^2 - \left(\beta_G^g\right)^2 \tag{4}$$

Where β_C^f and β_G^f can be used to calculate the volume-weighted column length $\langle L \rangle_V$:

$$\langle L \rangle_V = \frac{\lambda}{\beta_C^f cos\theta}$$

and the microstrain (ε)

$$\varepsilon = \frac{\beta_G^f}{4tan\theta}$$

This method can be applied when only a first order reflection can be measured. However it must be used carefully, since the size-broadened profile is assumed to be Gaussian and the strain broadened profile Lorentzian. Single-Line methods must be used only when no other options are available [12].

3.2. Warren-Averbach Method

By the kinematical theory of X-ray diffraction the physical profile of a Bragg reflection is given by the convolution of the crystallite size and the microstrain profiles [13]. The application of Fourier Transform on the physical profile allows separating these two contributions and this method is known as the Bertaut-Warren-Averbach Method or simply Warren-Averbach Method:

$$lnA\left(L, \frac{1}{d}\right) = lnA^S(L) - 2\pi^2 \langle {\varepsilon_L}^2 \rangle L^2/d^2$$

where L is the Fourier Length, defined as $L = n.a_3$, where $a_3 = \lambda/2(sin\theta_2 - sin\theta_1)$, n is the harmonic number, θ_1 is the initial angle of the peak, θ_2 is the final angle of the peak, d is the interplanar spacing and $\langle {\varepsilon_L}^2 \rangle$ stand for mean squared strain [14].

In this work the above equation was plotted for the interplanar spacing corresponding to the (101) and (202) reflections of the Zircaloy samples. This procedure allows separating the size (linear coefficient) and microstrain (slope) contributions from the linear curve. To calculate the mean crystallite sizes, the values of $A^S(L)$ against L were plotted, where the intercept of the initial slope on the L-axis gives the area-weighted column length $\langle L \rangle_A$ [14].

3.3. Differences in the types of microstrains and mean crystallite sizes

As shown in previous works [15,16] the mean crystallite sizes and microstrain parameters are not defined in the same way; they vary according to the method used to calculate them. The single-line method, where a Voigt shaped peak is assumed, provides the volume-weighted column length and the maximum ("upper") strain [17], that can be defined as a root-mean-square (RMS) value of strain [18] if a Gauss strain distribution it is assumed.

$$\varepsilon_{RMS} = \sqrt{\frac{2}{\pi}}\varepsilon$$

The Warren-Averbach method provides the area-weighted column length and, therefore, the mean squared strain, assuming that the strain distribution is either Gaussian or very small [17].

3.4. Instrumental Correction and Standard Materials

For the Warren-Averbach method the instrumental contribution is corrected by the Stokes method [14]. This correction is performed in Fourier space by deconvoluting the standard profiles from the corresponding sample profiles. In the Single-Line method, where the profiles are approximated by a Voigt function, we used Eqs. (3) and (4).

To correct of the instrumental contribution to the profile breadths and to assess the influence of the standard on the results, we employed two types of standard materials. One of the standards was a standard reference sample of Y_2O_3 produced at IPEN [7]. This material was certified as having large and homogeneous crystallites and negligible microstrain [7], but for a meaningful correction it is necessary to choose its XRD reflections at an angular domain close to the ones where the reflections of the material under study appear and shift then accordingly. We can consider this standard as an ideal one with reflections at non-ideal angles.

We also tested the sintered Zircaloy sample as standard for the instrumental breadth. Due to the sintering process this sample presents negligible microstrains and reasonably high crystallite sizes and consequently, their diffraction profiles are very narrow. Therefore, the sintered Zircaloy is suited for the determination of the instrumental contribution to the experimental XRD profile breadth since the reflections of both standard and material under analysis are at the same Bragg angle. In this case we can consider this standard as a non-ideal standard with reflections at ideal angles.

The results for mean crystallite sizes and microstrains using both standard materials are presented and discussed in the following sections.

4. RESULTS AND DISCUSSION

As it can be seen in Fig. 3, the profile of the sintered Zircaloy is narrow and symmetric but more broadened than the profile of the ideal standard.

In Fig. 4 is shown, as example of the Warren-Averbach method, the plot of $\ln[A(L)]$ versus $1/d^2$ for some values of L for the "as-cast" Zircaloy sample using the sintered Zircaloy as standard. It was previously explained that this graph allows the separation of the contributions of mean crystallite size and RMS microstrain from the Fourier coefficients.

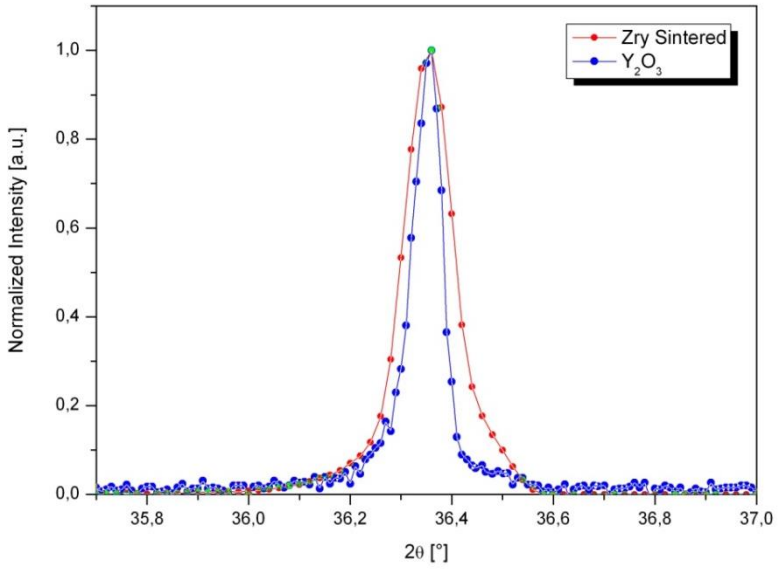

Figure 3: Diffraction peaks of the Zry SINT and Y_2O_3 standards used to correct the instrumental contribution.

In Fig.5 are shown the plots for the Fourier coefficients related to the size, $A^S(L)$ versus L for the Zircaloy sample REC, using as standards the Zircaloy SINT (a) and Y_2O_3 (b). When using the Zircaloy SINT as standard, the plot presents an asymptotic behavior for $L \rightarrow 0$, known as "hook effect" [14], due the fact that is a non-ideal standard. The correction of this effect is done by fitting a straight line to the almost linear part of the curve and normalizing the maximum value to 1. For both plots, the hook effect-corrected of Fig. 5(a) and the one of Fig. 5(b) we can fit a straight line to the almost linear part of the plot. The intercept of this line with the L axis gives the area-weighted column length $\langle L \rangle_A$.

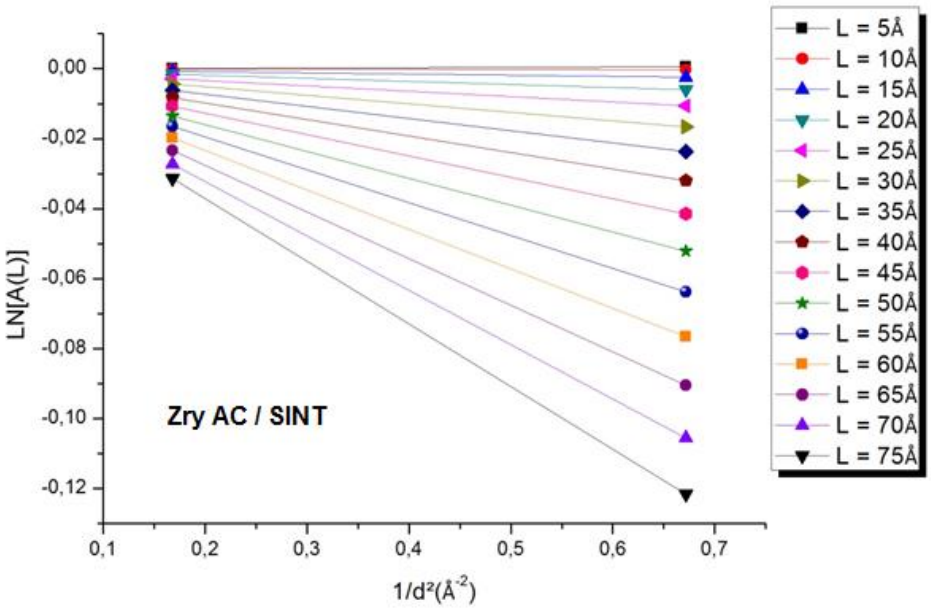

Figure 4: Separation of size and the microstrain contributions in the Fourier coefficients for the Zry AC sample.

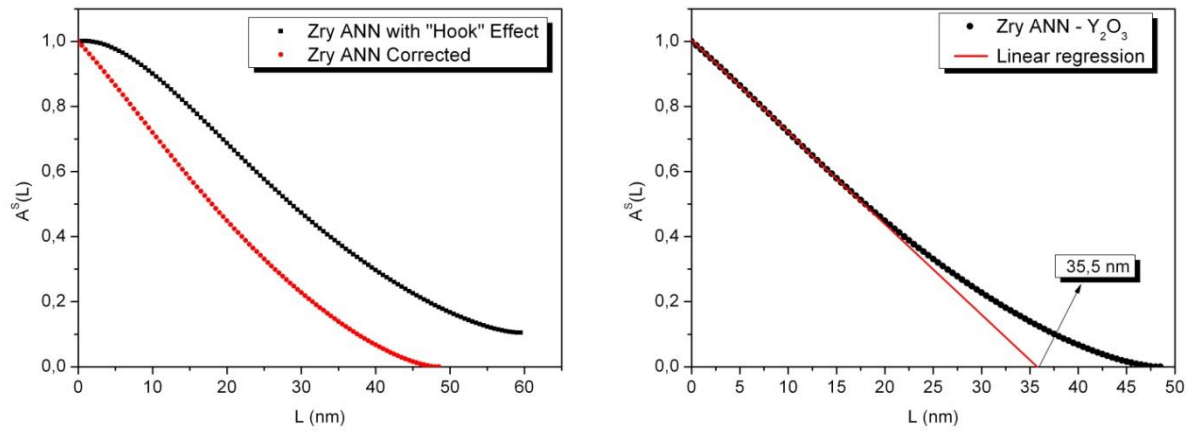

Figure 5: Plots for the (a) Fourier coefficients related to the size with (black) and without (red) Hook effect correction versus L; (b) Linear fit for the determination of the area-weighted column length $\langle L \rangle_A$.

In Table 1 are presented the results of $\langle L \rangle_A$ and $\langle \varepsilon(L)^2 \rangle^{1/2}$ for the VAR-remelted Zircaloy samples AC (as-cast), ANN (annealed) and TEMP (tempered), using both Zircaloy SINT and Y_2O_3 as standard for the instrumental correction.

Table 1 – Values for $\langle L \rangle_A$ and $\langle \varepsilon(L)^2 \rangle^{1/2}$ for the Zircaloy samples, using Zry SINT and Y_2O_3 as standard for the instrumental correction.

Zry	SINT		Y_2O_3	
	$\langle L \rangle_A$ (nm)	$\langle \varepsilon(L)^2 \rangle^{1/2}$ (10^{-4})	$\langle L \rangle_A$ (nm)	$\langle \varepsilon(L)^2 \rangle^{1/2}$ (10^{-4})
AC	7.9	9.5	7.9	13.7
ANN	36.6	0*	35.5	0*
TEMP	14.2	8.9	13.0	9.4

*Set to zero when $\langle \varepsilon(L)^2 \rangle$ is a small negative number.

The results for mean crystallite sizes and RMS microstrains, determined by using any of those two standards for correct the instrumental contribution, did not show significant differences. The values for mean crystallite sizes and RMS microstrains show that the as cast sample presents lower crystallite size and higher microstrain whereas the annealed sample presents higher crystallite size and no microstrain at all. The tempered sample presents intermediary values compared to the other samples. This behavior is compatible with the expected properties for the three samples.

Mean crystallite sizes and microstrains of AC sample show the typical behavior for a metal solidified from the melt, where high level of crystal defects and small crystallites are expected. Conversely, for the ANN sample, due to the recrystallization process, mean crystallite sizes are expected to be higher and microstrain values lower. The TEMP sample, which undergoes a phase transition from β to α when quenched from the treatment

temperature to ambient, presents mean crystallite sizes slightly higher than the AC sample but lower than in ANN sample. However the microstrains are of the same magnitude.

The results for mean crystallite sizes using both standard materials to correct instrumental breadth are similar for all samples but the results for microstrains are higher when an ideal standard is used, except for null microstrains. This can be explained by the overestimation of the instrumental breadth when the non-ideal standard is used and, consequently, the structural breadth is underestimated. The results for mean crystallite sizes are less influenced by the type of standard employed than microstrains. However, regardless of the standard used for the instrumental breadth correction, both sets of results can be considered as equally good estimations for mean crystallite sizes and microstrains.

In the case of Single-Line method (Fig. 6) the microstrains values obtained, displayed in Tab. 3 are unexpected. This can be explained by the fact that the microstrain cannot be satisfactorily represented by a Cauchy type function as required by the method. The values for the mean crystallite sizes although are as expected, which confirms the fact that sintered materials are good enough to estimate mean crystallite sizes when no standards are available.

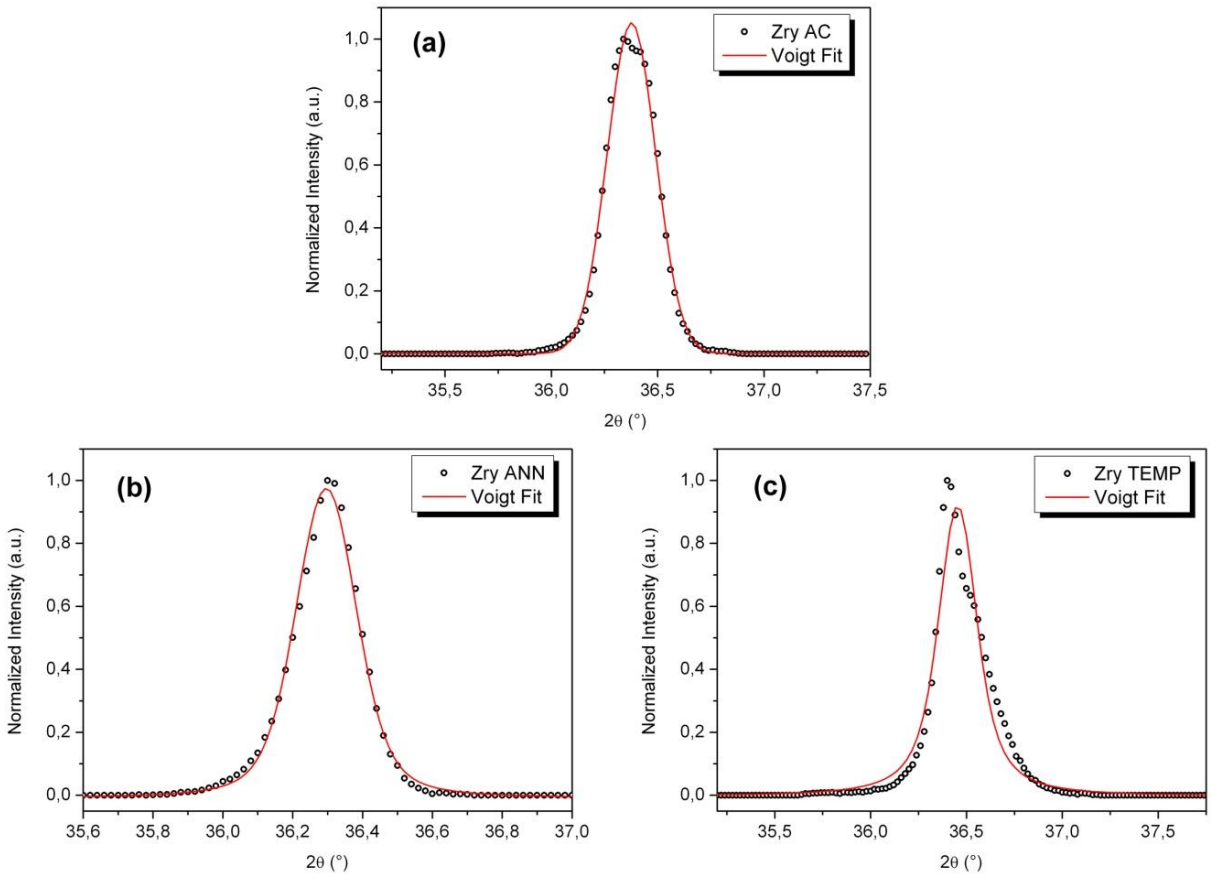

Figure 6: Voigt fits for (a) As-cast VAR-remelted sample; (b) annealed sample and (c) tempered sample for the application of the Single-Line method.

Table 2 – Values for $\langle L \rangle_V$ and $\langle \varepsilon(L)^2 \rangle^{1/2}$ for the Zircaloy samples using the Single-Line method.

Zry	SINT		Y_2O_3	
	$\langle L \rangle_V$ (nm)	$\langle \varepsilon(L)^2 \rangle^{1/2}$ (10^{-4})	$\langle L \rangle_V$ (nm)	$\langle \varepsilon(L)^2 \rangle^{1/2}$ (10^{-4})
AC	35.5	7.2	37.7	0 *
ANN	82.6	14.0	95.2	2.4
TEMP	25.3	2.8	26.4	0 *

The mean crystallites sizes and microstrain values for the sample SINT were estimated using the Single-Line method. A value of 92.9 nm was obtained for crystallite size and a negative microstrain value, which indicates that the sample neither has microstrain nor the Gaussian function considered is adequate to represent the microstrain contribution. The Warren-Averbach method was not applied due to the circumstance that very narrow peaks cause instability in the Fourier coefficients when the Stokes method is applied.

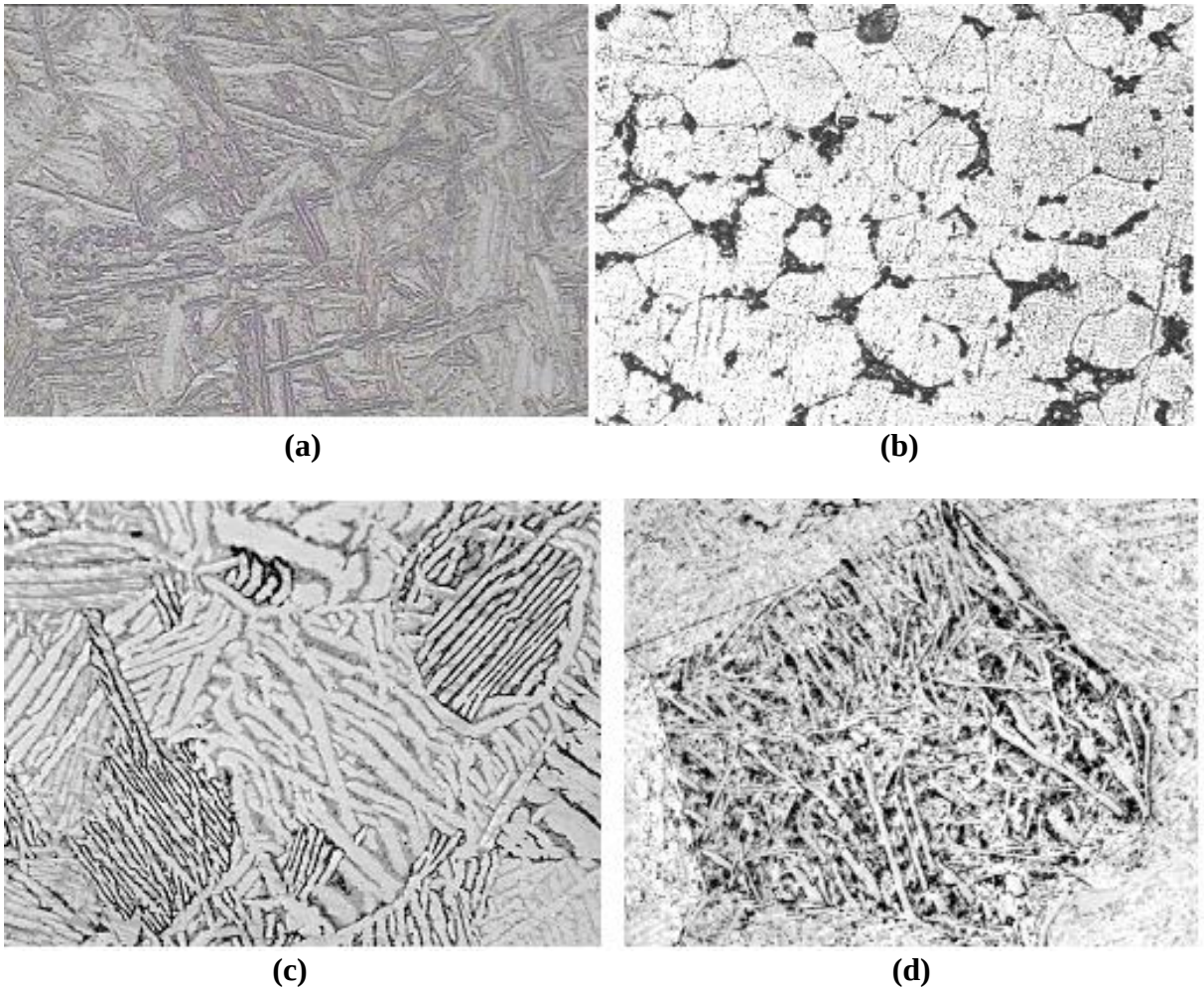

(a) **(b)**

(c) **(d)**

Figure 7: Optical micrographs for recycled Zircaloy samples. (a) As-cast VAR-remelted sample; (b) sintered sample; (c) annealed sample and (d) tempered sample.

Figure 6 shows the optical micrographs of the four kinds of samples, which can be matched with the results of Tab. 1. For the sample AC (a) the microstructure presents typical morphology of a metal solidified from melting, with dendritic grains , hence microstrains effects are expected. For the sample SINT (b), as the sintering time is long enough to allow high recrystallization, the grains are large and a low density of defects are foreseeable as well none or negligible microstrain. For the sample ANN (c) the microstrain is expected to be very low and the crystallite size high. Sample TEMP (d), who undergoes a phase transition from β to α on quenching, behaves as expected. Microstrains values are similar to the ones found in "as-cast" while crystallite sizes are higher than for "as-cast" but lower than for the "annealed" sample.

In Tab. 3 the values of hardness measured by two different hardness scales are presented: Marthens hardness (HM) and Vickers hardness (HV). For the three different heat-treated samples both matrix and lamellar phases hardness were measured. The samples obtained through VAR-remelting process presented the so-called "basketweave" microstructures, which is composed by a structure of lamellae in a matrix, as can be seen in Fig. 6. For sintered sample only homogeneous type of microstructure was observed. The results for hardness are in accordance with the results of microstrains presented in Tab. 1, confirming that the hardness, a macroscopic property, is closely related to the microstrains due to the crystal defects.

Table 3 – Measured values of Marthens and Vickers hardness for matrix and lamella phases in recycled Zircaloy samples from different processes.

Sample	**As-cast**		**Annealed**		**Tempered**		**Sintered**
Phase	Matrix	Lamella	Matrix	Lamella	Matrix	Lamella	-
Martens Hard. (HM)	3166	3567	2598	4128	3181	3810	4159
Vickers Hard. (HV)	424	493	330	591	422	545	599

5. CONCLUSIONS

The results discussed along this contribution allow concluding that the Warren-Averbach XPLA method is a powerful tool for studying the microstructure of materials. This method is capable of accurately determine mean crystallite sizes and microstrains, therefore permitting to explain the macroscopic properties of the studied materials. The Single-Line XLPA method, although less reliable, especially for microstrains determinations, can be used as alternative method when it is not possible employ W-A method. Also, it can be concluded that the use of a non-ideal standard, of the same material, for the correction of instrumental breadth in XLPA analysis can lead to an underestimation of microstrains and mean crystallite sizes, although being less sensitive in this latter case. Even if the use of an ideal standard can be considered more advisable, the differences in the results are not so substantial, which paves the path to use non-ideal standards as approach for adequate microstructural estimations.

ACKNOWLEDGMENTS

The authors acknowledge to CNEN for the scholarships of R.U. Ichikawa and L.A.T. Pereira, to CNPq (contracts n° 306530/2010-4 and 483686/2010-7) for financing part of this work and to FINEP.

REFERENCES

1. Sato, I. M.; Pereira, L. A. T.; Scapin, M. A.; Cotrim, M. B.; Mucsi, C. S.; Rossi, J. L.; Martinez, L. G. "Chemical and microstructural characterization of remelted Zircaloy by X-ray fluorescence techniques and metallographic analysis". *Journal of Radioanalytical and Nuclear Chemistry (Print),* **v. 1**, p. 1-6 (2011).
2. Martinez, L. G.; Pereira, L. A. T.; Takiishi, H.; Sato, I. M.; Salvador, V. L. R.; Soares, E. P.; Rossi, J. L. "Recycling of Zircaloy from nuclear fuel fabrication scraps". In: A. Mendez-Vilas (Org.). *Fuelling the Future: Advances in Science and Technologies for Energy Generation, Transmission and Storage*. 1ed. Boca Raton: Brown Walker Press, v. 1, p. 434-439 (2012),
3. Martinez, L. G.; Pereira, L. A. T.; Rossi, J. L.; Takiishi, H.; Sato, I. M.; Scapin, M. A.; Orlando, M. T. D. "Chemical and microstructural characterization of recycled zircaloy". In: *International Nuclear Atlantic Conference (INAC 2011)*, 2011, Belo Horizonte, MG. Trabalhos do INAC 2011. Rio de Janeiro: ABEN, 2011. v. 1. p. 1-15 (2011).
4. Takiishi, H.; Duvaizen, J. H.; Sato, I.M.; Rossi, J.L.; Pereira, L.A.T.; Martinez, L. G. "Recycling of Zircaloy Machining Chips by VAR Remelting and Powder Metallurgy Techniques". *Materials Science Forum* (Online), **v. 727-728**, p. 356-361 (2012).
5. Martinez, L. G.; Pereira, L. A. T.; Takiishi, H.; Sato, I. M.; Salvador, V. L. R.; Soares, E. P.; Rossi, J. L. "Recycling of Zircaloy from nuclear fuel fabrication scraps". In: *Energy and Materials Research Conference EMR2012, 2012*. Torremolinos, Spain, 20-22 Jun. *Book of Abstracts*. Málaga: FORMATEX, v. 1. p. 299-299 (2012).
6. Sato, I. M.; Pereira, L. A. T.; Scapin, M. A.; Cotrim, M. B.; Mucsi, C. S.; Rossi, J. L.; Martinez, L. G. "Chemical and microstructural characterization of remelted Zircaloy by X-ray fluorescence techniques and metallographic analysis". In: *Fourth International Symposium on Nuclear Analytical Chemistry (NAC-IV)*, 2010, Mumbai, India. *Proceedings of the Fourth International Symposium on Nuclear Analytical Chemistry (NAC-IV).* Mumbai, INDIA: Bhabha Atomic Research Center (2010).
7. Martinez, L. G.; Orlando, M. T. D.; Corrêa, H P S; Ferreira, F, F.; Paiva-Santos, C. O.
"Production of standard reference samples for powder diffraction" In: *18º Congresso Brasileiro de Engenharia e Ciência dos Materiais*, 2008, Porto de Galinhas, PE.
Resumos do 18 CBECiMat. São Paulo (2008).
8. Balzar, D.: "Voigt-function model in diffraction line-broadening analysis". In R. L. Snyder, H. J. Bunge, and J. Fiala. *Microstructure Analysis from Diffraction*. International Union of Crystallography (1999).
9. Balzar, D.: "Profile Fitting of X-ray Diffraction Lines and Fourier Analysis of Broadening". *J. Appl. Cryst*. **25, p.** 559 – 570 (1992).
10. de Keijser, Th. H.; Langford, J. I.; Mittemeijer, E. J.; Vogels, A. B. P.: "Use of the Voigt function in a single-line method for the analysis of X-ray diffraction line broadening". *J. Appl. Cryst.* **15, p.** 308–314 (1982).
11. Delhez, R.; de Keijser, Th. H.; Mittemeijer, E. J.: "Accuracy of Crystallite Size and Strain Values from X-ray Diffraction Line Profiles using Fourier Series". In Block, S.; Hubbard, C.

R.: *Accuracy in Powder Diffraction*. National Bureau of Standards, Washington, DC. 213 – 253 (1980).
12. Krill, C. E.; Haberkorn, R., Birringer, R.: "Specification of Microstructure and Characterization by Scattering Techniques". In Nalwa, H. S.: *Handbook of Nanostructured Materials and Nanotechnology*. Vol. 2: Spectroscopy and Theory. Academic Press (2000).
13. Langford, J. I.: "A Rapid Method for Analysing the Breadths of Diffraction and Spectral Lines using the Voigt Function". *J. Appl. Cryst*. **11,** p. 10-14 (1978).
14. Lucks, I.; Lamparter, P.; Mittemeijer, E. J.: "An evaluation of methods of diffraction-line broadening analysis applied to ball-milled molybdenum". *J. Appl. Cryst*. **37**, p. 300-311 (2004).
15. Rane, G. K.: "Microstructure and grain growth of nanosized materials". Dissertation an der Universität Stuttgart. Max Planck Institut für Intelligente Systeme (ehemals Max Planck Institut für Metallforschung) Stuttgart (2012).
16. Santra, K.; Chatterjee, P.; Sen Gupta, S. P.: "Voigt modelling of size-strain analysis: Application to α-Al_2O_3 prepared by combustion technique". *Bull. Mater. Sci*., Indian Academy of Sciences. **Vol. 25**, No. 3, p. 251-257 (June 2002).
17. Ungár, T.: "Microstructure Parameters from X-ray Line Profile Analysis". In Singh, A. K.: *Advanced X-ray Techniques in Research and Industry*. India (2005).
18. Ungár, T.: "The Microstructure in Terms of Dislocations and Size-Distribution from X-ray Diffraction Analysis". In Gupta, S. P.; Chatterjee, P.: *Powder Diffraction, Proceedings of II International School on Powder Diffraction*. IACS, Kolkata, India (2002).
19. Warren, B. E.: "X-Ray Diffraction". Addison-Wesley, (Addison-Wesley Series in Metallurgy and Materials) (1969).